Hanbury Brown–Twiss interferometry of direct photons in heavy ion collisions

D. Peressounko*
RRC "Kurchatov Institute," Kurchatov sq., 1, Moscow, Russia
(Received 30 December 2001; revised manuscript received 31 July 2002; published 31 January 2003)

We explore the possibility of measurements of Hanbury Brown–Twiss correlations in $\gamma\gamma$ channels in the high multiplicity environment of heavy ion collisions. We consider all possible sources of photon-photon correlations and show that one can separate correlations of photons produced directly in the hot zone and residual correlations of decay photons: the former contribute to the region of small invariant relative momentum $q_{inv} \lesssim 50$ MeV, while the latter contribute to larger relative momentum and, negligibly, to the small q_{inv} region. We make predictions of the photon correlation functions at SPS and RHIC energies.

DOI: 10.1103/PhysRevC.67.014905 PACS number(s): 25.75.Gz

I. INTRODUCTION

Hanbury Brown–Twiss (HBT) interferometry is known to be a powerful tool to explore space-time dimensions of the hot zone created in elementary particle or heavy ion collisions. Historically such measurements have concentrated on pion correlations. However, recently they have been applied to kaons, protons, and even heavy fragments [1]. Hadronic correlations reflect the space-time extent of the source at freeze-out time. An important complementary information can be obtained from photon-photon correlations. In contrast to hadrons, photons are emitted mostly from the central hot zone and reflect the history of the hottest part of the collision. Moreover, photons are not influenced either by strong or by Coulomb final state interactions; therefore, HBT parameters can be measured in the photon channel with smaller systematic error.

Unfortunately photon interferometry is faced with considerable difficulties compared to hadron interferometry, as a consequence of the small yield of photons emitted directly from the hot zone and of the strong background due to electromagnetic decay of final hadrons. That may explain why up to now there have been only a few experimental investigations of photon-photon correlations in heavy ion collisions [2].

The importance of the photon interferometry to study the history of heavy ion collisions has been stressed several times [3,4], where *direct* photon correlation functions were considered in the frame of 1+1 and 3+1 scaling hydrodynamics. It was shown that transverse radii R_s and R_o deduced from photon correlation functions are sensitive to the history of the collision and the longitudinal radius R_l is up to one order of magnitude smaller than $R_s \sim R_o$ — in contrast to hadron correlations, where all three radii are approximately equal. This difference of radii was attributed to the fact that thermal photons are emitted mostly from the very beginning of the collision when the temperature of the hot matter is maximal and the longitudinal size of the system is small.

Direct photon interferometry is certainly a very promising tool, but it is not clear how to measure these correlations in the experiment. In the high multiplicity environment of heavy ion collisions it is not possible to separate direct and decay photons on an event-by-event basis and construct correlations of direct photons only. In this paper we address the question of how to extract correlations of direct photons from correlations of *all* photons produced in the collision. We show that correlations of direct photons appear in the total photon correlation function at small relative momenta, while residual correlations of photons produced in the decay of correlated final hadrons appear only at larger relative momenta.

The paper is organized as follows. In Sec. II we present the expression for two-photon correlation function, accounting for the spin of photons, and discuss several parametrizations of it. In Sec. III we analyze possible sources of correlations of decay photons and demonstrate how they can be separated. In Sec. IV we outline a model of the evolution of hot matter. In Sec. V we apply this model to predict the shape of the photon correlation functions and HBT parameters for SPS and RHIC energies. Conclusions are formulated in Sec. VI.

II. CORRELATION FUNCTION OF DIRECT PHOTONS

The expression for the correlation function of two scalar bosons has been derived several times in the literature (see, e.g., [5]):

$$C_2(q,K) = 1 + \lambda \frac{\left| \int d^4x S(x,K) e^{iqx} \right|^2}{\left| \int d^4x S(x,K) \right|^2}, \qquad (1)$$

where $q = k_1 - k_2$ is the relative momentum of the boson pair, $K = (k_1 + k_2)/2$ is half of the total pair momentum, $S(x,K)$ is the Wigner density of the boson source, and λ the "strength of the correlations," equal to 1 for a fully chaotic source and 0 for a fully coherent source. The way to take into account the spin of photons has so far been rather confusing. It was first stated [6,7] that in the case of photons λ is changed by introducing a momentum-dependent term:

$$\lambda = \frac{1}{4}\left(1 + \frac{\vec{k}_1 \cdot \vec{k}_2}{|\vec{k}_1||\vec{k}_2|}\right), \qquad (2)$$

*Electronic address: Peressounko@cern.ch

where $\vec{k}_1$ and $\vec{k}_2$ are the three-momenta of the photons. Later it was shown [8] that an accurate treatment of the current conservation relations leads to another expression for the ''correlation strength,''

$$\lambda = \frac{1}{2}. \tag{3}$$

The latter approach was again criticized in [9] and expression (2) was retained. To clarify this situation one should first note that $C_2(q,K)$ is a Lorenz scalar, and so must be λ and ratio on the right-hand side (rhs) of Eq. (1). By definition λ is independent of the source sizes but only on its chaocity. Therefore it can depend only on the momenta of photons. It is impossible, however, to construct a dimensionless Lorenz scalar from two massless four-vectors; therefore, λ can only be a constant. Treating Eq. (23) of [8] in terms of Lorenz invariance, one finds that the tensors $S_{\mu\nu}(\mathbf{q},\mathbf{K})$ can only be $g_{\mu\nu}S(\mathbf{q},\mathbf{K})$, which gives the additional argumentation of their calculations leading to the correct expression for λ, Eq. (3), and removes objections of [9].

In the following we use the ''out-side-long'' Cartesian parametrization of the correlation function; i.e., we decompose the relative momentum of the pair $\vec{q}$ into ''out'' (q_o), ''side'' (q_s), and ''long'' (q_l) components, where q_o is the projection of the relative momentum onto the direction of the transverse total momentum, q_l is the longitudinal component of the relative momentum, and q_s is the projection of the relative momentum onto the third perpendicular direction.

From the experimental point of view it is much easier to extract the distribution over the invariant relative momentum $q_{inv}=\sqrt{-q^2}$. Although it was stressed several times that the corresponding correlation radius contains only averaged information about source space-time dimensions, such a distribution is a satisfactory first step toward the extraction of more precise information:

$$C_2(q_{inv},K) = \frac{P_2^c(q_{inv},K)}{P_2^{nc}(q_{inv},K)}, \tag{4}$$

where P_2^c and P_2^{nc} represent correlated and noncorrelated two-photon distributions, respectively. In the smoothness approximation $[P_1(K+q/2)P_1(K-q/2)\approx P_1^2(K)]$ and on-shell approximation ($K_0=|\vec{K}|$) we can write

$$P_2^c(q_{inv},K) = K_0\frac{dN}{dq_{inv}d^3K} = 2\frac{q_{inv}}{K_0}P_1^2(K)\int d^3q\,\delta(q_{inv}^2+q^2)C_2(q,K),$$

$$P_2^{nc}(q_{inv},K) = K_0\frac{dN}{dq_{inv}d^3K} = 4\pi\frac{q_{inv}^2}{K_0}P_1^2(K),$$

where $P_1(K)$ is the one-photon distribution.

From the above expressions one can see that the shape of the correlation function depending on q_{inv} differs from the shape of the $3d$ correlation function and therefore the ''correlation strength'' λ_{inv}, measured in this way may depend on the shape of the $3d$ correlation function as well.

III. PHOTON CORRELATIONS IN A HIGH MULTIPLICITY ENVIRONMENT

In relativistic heavy ion collisions it is not possible to separate direct photons from decay ones and calculate their correlation function on an event-by-event basis. Indeed, in a high multiplicity environment, for any photon there are a lot of candidates to construct a π^0. This has been seen in the invariant mass distribution of photon pairs measured in Pb+Pb collisions at SPS energy [10], where only a few percent of pairs with mass in the region of π^0 mass are indeed the product of the decay of the same pion. The two-photon correlation function measured in such environment will have the form

$$C_2(k_1,k_2) = \frac{P_2^{dd}(k_1,k_2)+P_2^{df}(k_1,k_2)+P_2^{ff}(k_1,k_2)}{[P_1^d(k_1)+P_1^f(k_1)][P_1^d(k_2)+P_1^f(k_2)]},$$

where $P_2^{dd}(k_1,k_2)$ is the two-photon distribution in which both photons are direct, $P_2^{df}(k_1,k_2)$ is the two-photon distribution in which one photon is direct and another is the product of decay of the final hadron, $P_2^{ff}(k_1,k_2)$ is the two-photon distribution in which both photons are products of the decay of final hadrons, and $P_1^d(k)$ and $P_1^f(k)$ are the contributions of direct and decay photons into the one-particle distribution, respectively. The first term of the numerator $P_2^{dd}(k_1,k_2)$ is the most interesting part of the correlation function; it is what we would like to extract. The second term in the numerator is nothing but the product of the one-particle distributions of direct and decay photons:

$$P_2^{df}(k_1,k_2) = P_1^d(k_1)P_1^f(k_2)+P_1^d(k_2)P_1^f(k_1).$$

Indeed, the emission points of two photons are separated at least by the lifetime of the final hadron and there is no dynamical correlations between direct photons and final hadrons. In contrast, the last term of the numerator may contain the residual correlations left in the products of the correlated hadrons. As far as the number of decay photons is much larger than the number of direct ones, even small residual correlations can make correlations of the direct photons unobservable. Because of its importance, we will consider this term later and show that its contribution is completely negligible for small $q_{inv}\lesssim 50$ MeV. As for the denominator, it does not change the shape of the correlation function, and the mixing of the direct and decay photons leads only to the decreasing of the ''correlation strength'' parameter.

Residual photon correlations.

In this subsection we consider the influence of the hadron-hadron correlations on the correlations of daughter photons. These can be Bose-Einstein correlations of final pions or kinematic correlations like those in the reaction $K_s^0\to 2\pi^0\to 4\gamma$.

For example, let us consider π^0-π^0 Bose-Einstein correlations. Assume that two pions with momenta p_1 and p_2 decay onto four photons with momenta k_1, k_2 and k_3, k_4. We can write for the invariant relative momentum $q=\sqrt{-(k_1-k_3)^2}$ the distribution of photon pairs (note that we do not consider trivial correlations of photons belonging to one pion):

$$\frac{dN^{\gamma\gamma}}{dq}=2\,q\int\frac{d^3k_1}{2\omega_1(2\pi)^3}\frac{d^3k_2}{2\omega_2(2\pi)^3}\frac{d^3k_3}{2\omega_3(2\pi)^3}\frac{d^3k_4}{2\omega_4(2\pi)^3}\times\delta(q^2+(k_1-k_3)^2)(2\pi)^4\delta^4(p_1-k_1-k_2)\times(2\pi)^4\delta^4(p_2-k_3-k_4)\frac{d^3p_1}{2\varepsilon_1(2\pi)^3}\frac{d^3p_2}{2\varepsilon_2(2\pi)^3}\times f(p_1)f(p_2)C_2(p_1,p_2), \tag{5}$$

where $f(p)$ is the distribution function of pions and $C_2(p_1,p_2)$ their correlation function. Performing calculations, presented in the Appendix, we find finally

$$\frac{dN^{\gamma\gamma}}{dq}=\frac{q}{2^7\pi^2}\int dQ\frac{dN^{\pi\pi}}{dQ}\frac{\theta(\varepsilon+p-q)}{p\varepsilon}\times\left\{\ln\left[\frac{\varepsilon+p}{\varepsilon-p}\right]+\min\left(0,\ln\left[\frac{\varepsilon-p}{q}\right]\right)\right\}, \tag{6}$$

where Q is the invariant relative momentum of the parent pions, $dN^{\pi\pi}/dQ$ is their distribution over this relative momentum, $p=Q/2$, and $\varepsilon=\sqrt{Q^2+4\,m^2}/2$. It is convenient to split the region of q into two subregions. First, $0<q\leqslant m$,

$$\frac{dN^{\gamma\gamma}}{dq}=\frac{q}{2^7\,\pi^2}\int_0^\infty dQ\,\frac{dN^{\pi\pi}}{dQ}\,\frac{1}{p\,\varepsilon}\ln\left[\frac{\varepsilon+p}{\varepsilon-p}\right]+\frac{q}{2^7\,\pi^2}\int_{(m^2-q^2/q)}^\infty dQ\,\frac{dN^{\pi\pi}}{dQ}\,\frac{1}{p\,\varepsilon}\ln\left[\frac{\varepsilon-p}{q}\right]. \tag{7}$$

Second, $q>m$,

$$\frac{dN^{\gamma\gamma}}{dq}=\frac{q}{2^7\,\pi^2}\int_{q-m^2/q}^\infty dQ\,\frac{dN^{\pi\pi}}{dQ}\,\frac{1}{p\,\varepsilon}\ln\left[\frac{\varepsilon+p}{q}\right]. \tag{8}$$

Our main objective in this section is to consider the behavior of the photon correlation function at small q. One can see that for $q<m$ the photon correlation function (6) consists of two terms. The first one is independent of q, while the second one depends on q through the integration limits and $\ln(q)$. Note that the lower limit of the integral increases to infinity with decreasing of q, so that its contribution vanishes.

As an illustration, we present the correlation functions of photons calculated for a simple parametrization of the pion correlation function,

$$C_2(Q_{inv})=\exp(-R_{inv}^2\,Q_{inv}^2),$$

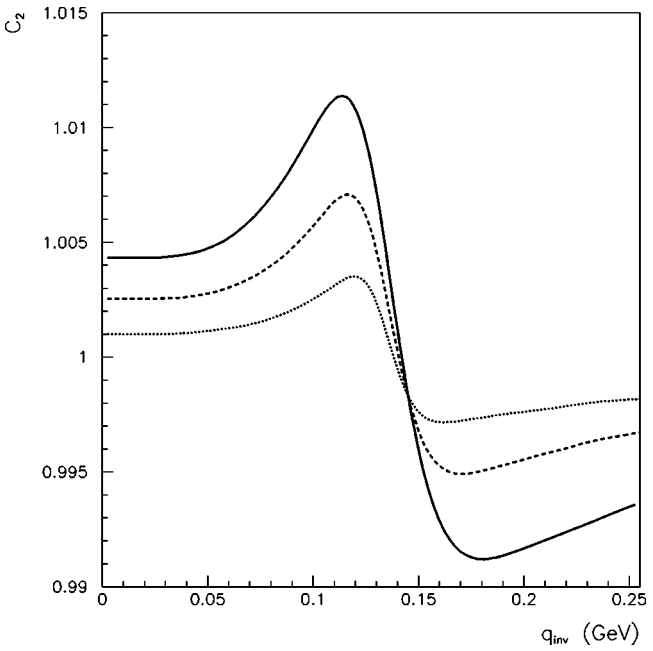

FIG. 1. Correlation functions for photons, produced by pions for three radii R_{inv} of the pion correlation function: 4 fm (solid line), 5 fm (dashed line), and 7 fm (dotted line).

and a Hagedorn-like p_T distribution and Gaussian rapidity distribution taken from WA98 data [10]; see Fig. 1. One can observe two important features of the distribution: First, for small relative momentum $q_{inv}\lesssim 50$ MeV the correlation remains constant, and second, the resulting complicated wavelike structure is completely different from the original pion correlation function. This behavior can be explained in the following way: consider two pions with zero relative momentum decaying into photons. For geometrical reasons the distribution over photon relative momentum will have the form

$$\frac{dN^{\gamma\gamma}}{dq}=\frac{\text{const}}{\sqrt{m^2-q^2}},$$

and the average relative momentum will be $<q_{inv}>=\frac{2}{3}m$. To populate smaller values of the photons relative momentum it is necessary to use *larger* values of the relative momentum of the pions: in this case, as a result of Doppler shift, half of the photons will be less energetic and one could build up smaller q_{inv}. This is why the photon correlation function deviates much strongly from unity above and *below* $q_{inv}=\frac{2}{3}m$ for the case of a wider pion correlation function.

Note that our conclusion differs from the conclusion made in [11], where it was stated that the correlation function of the decay photons reproduces the correlation function of the parent pions although with smaller ''correlation strength.'' The origin of the difference is cut on K_T of the daughter photons applied in [11]: selecting photons with almost the same K_T as parent pions, one chooses photons, preserving the correlation of parent pions. In contrast, in the present paper we consider a K_T-averaged correlation. Therefore, one could expect correlations, described by Eq. (6), for $K_T\lesssim m$

and repeating correlations of the parent pions for $K_T \gg m$. In addition, there is a trivial error in Eq. (5) of [11], where a wrong expression for phase space ρ was used: it lacks a factor $1/\omega$ for each decay photon, which leads to a small variation of the photon correlation function.

Another possible source of residual correlations of decay photons is decays of some hadrons onto several neutral pions, $X \to 2\pi^0 + X'$, or photons and neutral pions, $X \to \gamma\pi^0 + X'$. We consider the reactions $K_S^0 \to 2\pi^0 \to 4\gamma$, $\eta \to 3\pi^0 \to 6\gamma$, and $\omega \to \gamma\pi^0 \to 3\gamma$. As one can see, this list contains all possible types of reactions. To calculate the residual correlations of the decay of K_S^0 we substitute $dN^{\pi\pi}/dQ = Br_{K_S^0 \to 2\pi^0}\ \delta(Q - M_{K_S^0})$ into Eq. (6). For the case of correlations due to the decay of η, for the distribution of daughter pions, we have

$$\frac{dN^{\pi\pi}}{dQ} = \frac{\pi^2}{4\ M_\eta}\ \mathrm{Br}_{\eta \to 3\pi^0} \sqrt{Q^2 - 4\ m_\pi^2} \times \sqrt{Q^4 - 2\ Q^2\ (M_\eta^2 + m_\pi^2) + (M_\eta^2 - m_\pi^2)^2}, \quad (9)$$

where M_η is the mass of the η meson and m_π is the mass of π^0.

Finally, calculating the photon correlations in the decay $\omega \to \gamma\pi^0 \to 3\gamma$, one finds

$$\frac{dN}{dq} = \frac{4\ q}{M_\omega^2 - m_\pi^2}\ \mathrm{Br}_{\omega \to \pi^0\gamma}\ \theta\left(\sqrt{M_\omega^2 - m_\pi^2} - q\right). \quad (10)$$

To construct correlations function from Eqs. (9) and (10) one needs a combinatorial background. For demonstration purposes we took the same background as for the calculation of residual correlations in decays of Bose-Einstein correlated π^0. The resulting correlations functions, normalized to one parent resonance (K_S^0, η, ω) per event, containing 200 neutral pions in midrapidity, which roughly corresponds to Pb+Pb collisions at SPS, are presented in Fig. 2. As one can see from this figure, neither one of the contributions produces an increase in the small-Q_{inv} region. In addition, the strength of the corresponding correlations is extremely small, and therefore they can be neglected in the analysis. As far as decay photons having a steeper slope than products of decays of directly produced pions, we estimated an upper limit on these correlations and one could expect a decreasing of the strength of these correlations with an increasing of K_T.

Another important issue of Eq. (7) is that one can measure the correlation function of neutral pions in the two-photon channel. This is favorable with respect to the measurement of this correlation function in the 4γ channel because in the latter there is a huge combinatorial background, considerably influenced by kinematic effects [12]. However, a discussion of the possibility of the measurement of π^0 correlations is outside the scope of the current paper and will be published elsewhere [13].

A last point to end the discussion: what will happen if we return from the averaged correlation function $C_2(q_{inv})$ to the correlation function depending on three components of the relative momentum of the photon pair $C_2(q_o, q_s, q_l)$? In the case of OSL parametrization and the local comover system (LCMS), we find $q_{inv}^2 = q_o^2 + q_s^2 + q_l^2$, which means that the correlation function expressed in terms of components of the relative momentum will be undistorted at least within some sphere, determined by radius $q_{inv} \sim 50$ MeV.

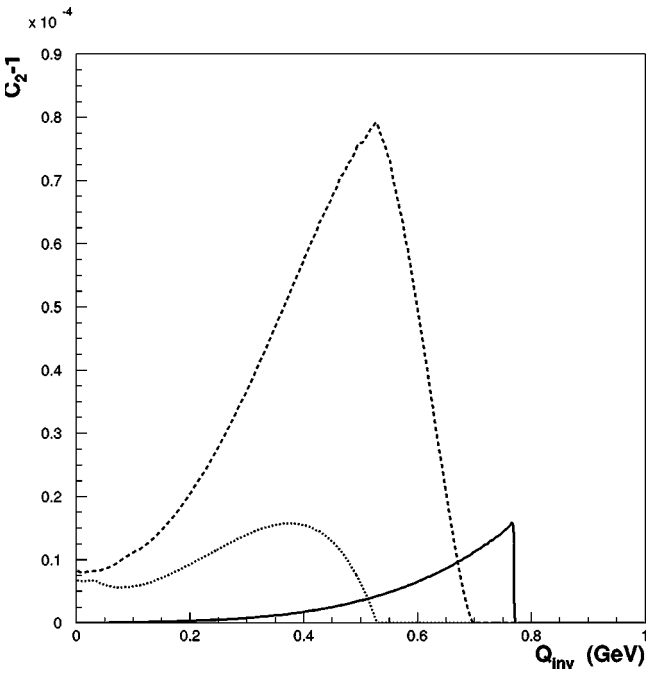

FIG. 2. Correlation functions of photons, originated in decay $K_S^0 \to 2\pi^0 \to 4\gamma$ (dotted line), $\eta \to 3\pi^0 \to 6\gamma$ (dashed line), and $\omega \to \gamma\pi^0 \to 3\gamma$ (solid line).

IV. DYNAMICS OF THE *AA* COLLISION

We describe the evolution of the collision on the basis of the hydrodynamic model. Having described the evolution, we calculate the yield and emission pattern of thermal photons. We account also for the contribution of prompt photons produced on the preequilibrium stage of collision and decay photons.

In this paper we do not consider the details of the preequilibrium dynamics of heavy ion collisions. Instead we use a simple model to estimate the influence of prompt photons on the photon correlation parameters. We assume that the emission points of prompt photons are distributed in the transverse direction following a Woods-Saxon distribution integrated along the beam axis and constant in the longitudinal direction, while the length of the emitting region linearly increases with time. We assume that the emission rate of prompt photons from a unit volume is constant and independent of time. The value of this emission rate is chosen to reproduce the total yield of prompt photons, evaluated using perturbative QCD-inspired parametrization of the experimental data from pp and pA collisions — for details see [14].

Hydrodynamic evolution of the thermalized hot matter is described in the frame of 3+1 scaling hydrodynamics with cylindrical symmetry. To fix the model one has to specify the equation of state (EOS) of hot matter and choose values of

the free parameters, such as the shape of the initial energy and velocity profiles, initial temperature T_{in}, initial time τ_{in}, transition temperature T_c — if a phase transition is assumed — and freeze-out temperature T_{fr}. We use two alternative equations of state, one with a first-order phase transition from an ideal partonic gas (QGP) with 2.5 quark flavors to the ideal gas consisting of all known mesons with masses below 2 GeV and baryons with masses below 3 GeV (bag model) and second EOS of an ideal hadronic gas without a phase transition. For each kind of EOS we fix initial conditions so that we reproduce the measured p_t distributions of neutral pions and direct photons. To calculate the p_t distributions of final hadrons, we take into account the decays of all heavier resonances. We fix the transition temperature $T_c = 170$ MeV and freeze-out temperature $T_{fr} = 120$ MeV.

We use the emission rate of thermal photons from the QGP, accounting for Compton scattering and annihilation [15] and near-collinear bremsstrahlung and inelastic pair annihilation contributions, with the incorporation of Landau-Pomeranchuk-Migdal suppression [16]. For the emission from the hadronic gas we use the emission rate, accounting for the contribution of reactions $\pi\rho \to \pi\gamma$, $\pi\pi \to \rho\gamma$, etc. [15], and the important contribution from the reaction $\pi\rho \to a_1 \to \gamma\pi$ [17]. The lifetime of the a_1 meson is rather small, $\tau = 0.3$–1 fm/c; therefore, we neglect the smearing of the position of the emitting of photon.

V. HBT PARAMETERS AT SPS AND RHIC

In this section we estimate the visibility of the direct photon correlations in heavy ion collisions and make predictions for the HBT parameters at SPS and RHIC energies. We repeat existing calculations [3,4] because the emission rates of the QGP and hadronic gas were reevaluated since that time and changed considerably, which could influence HBT radii. In addition, we account for contribution of the preequilibrium stage of the collision and remove freedom in choosing the initial conditions for the hydrodynamic model, requiring a reproduction of the π^0 spectrum and spectrum of direct photons measured in the Pb+Pb collisions at SPS energy [10] and $\pi^{\pm}$, π^0 spectrum in Au+Au collisions at RHIC [18].

To begin with we apply our model of evolution for the description of the SPS data. We find that it is possible to reproduce π^0 and direct photon spectra simultaneously within the EOS both with and without a phase transition. In the case of the EOS including the transition to the QGP phase we use $T_{in} = 360$ MeV and $\tau_{in} = 0.3$ fm/c, while in the case of the pure hadronic scenario we use $T_{in} = 250$ MeV and $\tau_{in} = 0.5$ fm/c.

Evolution of the energy density in midrapidity in Pb+Pb collisions at SPS energy, calculated with the EOS incorporating phase transition, is presented in Fig. 3. As far as we reach the EOS of the hadronic gas, the difference between degeneracy of the QGP phase and hadronic gas is relatively small, and therefore the lifetime of the mixed phase is much smaller than that of the hadronic gas and even of the QGP phase.

Having an emission pattern of direct photons we evaluate their correlation function. We calculate it in the local comover system as a function of four variables: $C_2(q_o, q_s, q_l, K_T)$. For each given value of K_T we fit slices $C_2(q_o,0,0,K_T)$, $C_2(0,q_s,0,K_T)$, and $C_2(0,0,q_l,K_T)$ with a function $1+\lambda\exp(-q_i^2 R_i^2)$ and find the dependences of radii $R_i(K_T)$ and $\lambda(K_T)$, shown in Figs. 4, 5, and 6, correspondingly. Comparing the contributions of different phases, we find that the correlation function of direct photons emitted in preequilibrium and the QGP phase (marked QGP in Fig. 4) has no K_t dependence and reflects just the average space-time dimensions of the region occupied by the QGP. In contrast, the mixed phase and to a larger extent the hadronic phase exhibit a K_t dependence which is a signal of considerable flow. As for typical values of the radii, R_o and R_s of the mixed phase are smaller and R_l is larger than those of the QGP phase, which is in accordance with Fig. 3, where the mixed phase occupies the volume of smaller radius but larger length. As for the hadronic gas contribution, it demonstrates that the hadronic gas occupies a volume with the largest transverse and longitudinal sizes and largest flow. Comparing the correlation strength parameters one can conclude that the contribution of the mixed phase is negligible; the hadronic phase dominates at $K_t \lesssim 2$ GeV and the QGP above $K_t \sim 2$ GeV. Note that when constructing the correlation function of all direct photons in the event, one should add the amplitudes of all these contributions, and a strong interference between them might appear. In the region, where the ''correlation strength'' parameters of the contributions of the QGP and hadronic phase are comparable ($K_t \sim 2$ GeV), we observe a two-component structure of correlation functions, depending on Q_o and Q_l projections of the relative momentum. This effect was first found in [19], where it was pointed out that it could be used as a signal of the phase transition, and moreover, one thus can measure the lifetime and sizes of the QGP phase.

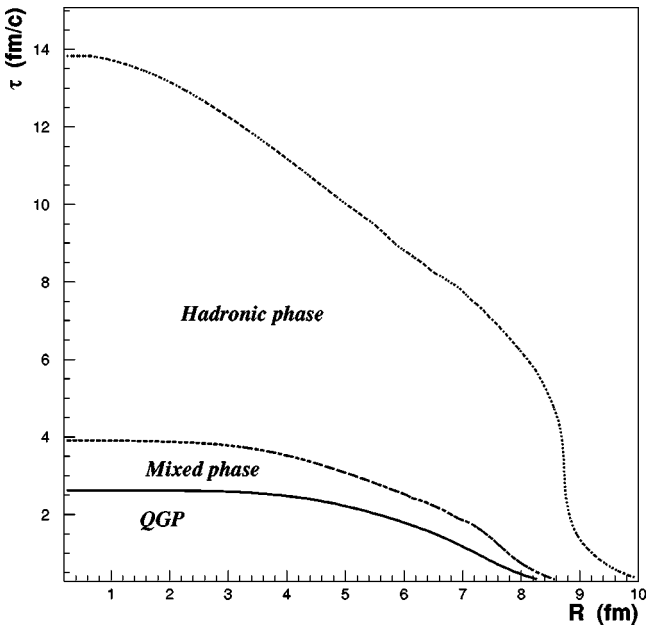

FIG. 3. Levels of constant energy density in midrapidity in Pb+Pb collisions at SPS energy.

Comparing the HBT radii of direct photon correlations

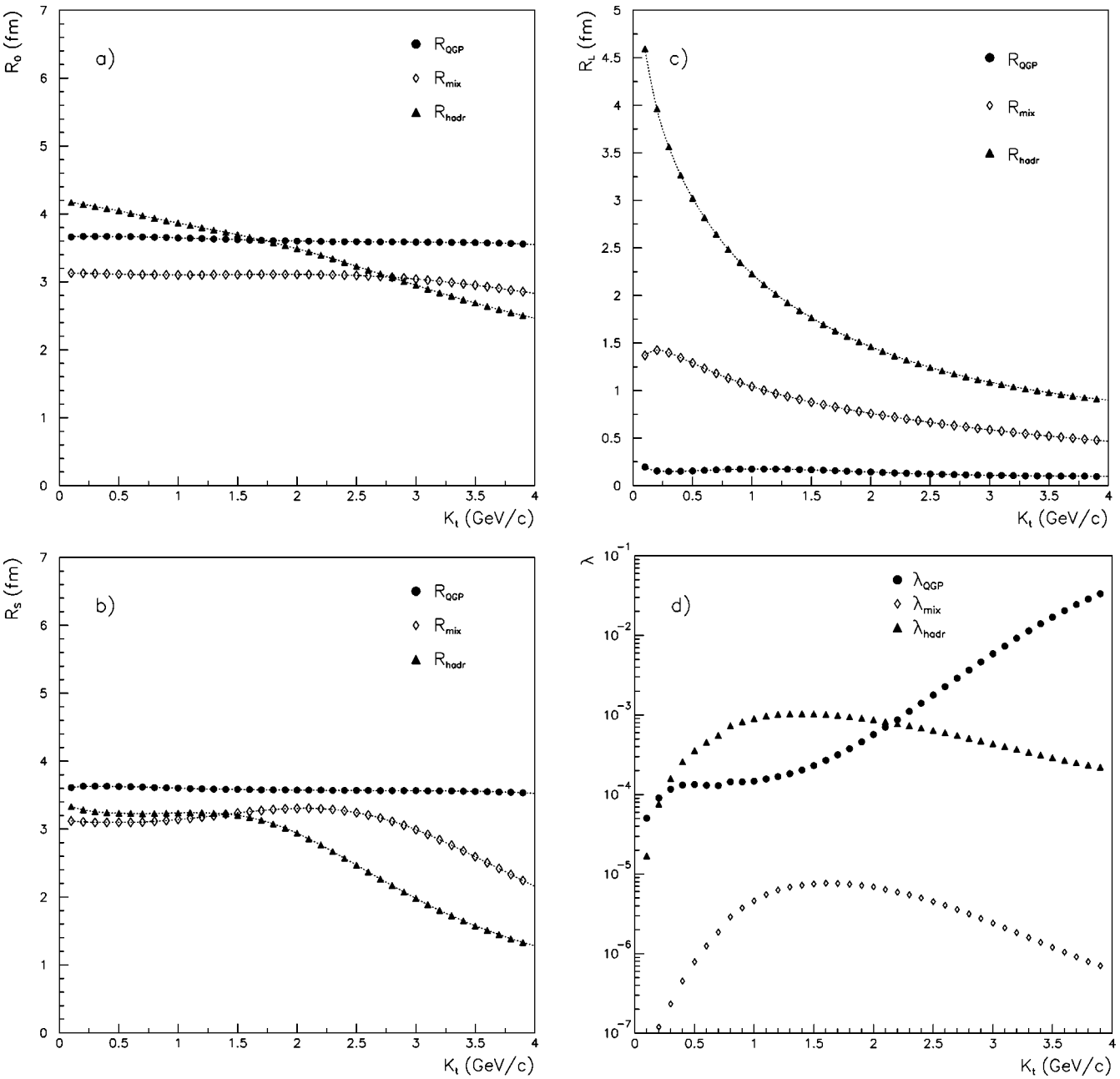

FIG. 4. Comparison of correlation radii in *out*, *side*, and *long* directions [plots (a), (b), and (c), correspondingly] and "correlation strength" parameters [plot (d)], obtained by fitting contributions of the QGP, mixed, and hadronic phases into the direct photon correlation function.

calculated for two possible EOS (see Fig. 5), we find that the radii are rather similar in both cases. This is in contrast with expectations that due to the longer evolution of the system experiencing a first-order phase transition, the HBT radii should considerably differ. As a result of the inclusion of a large number of resonances into the EOS of the hadronic gas, the effective degeneracy of the hadronic gas at the phase transition temperature $g_{hadr} \approx 25$ is close to the degeneracy of the QGP, $g_{QGP}=42$, and therefore the influence of the mixed phase on the lifetime is rather small. The lifetime of the system is defined mainly by the expansion rate, which in turn depends on the speed of sound in the given phase, which is smaller in the hadronic phase: the lifetime of hot matter in the case of a pure hadronic gas EOS, $\tau_{hadr}=15$ fm/c, is even larger than the lifetime of hot matter with the EOS including the phase transition, $\tau_{QGP}=14$ fm/c.

The decreasing of R_o and increasing of R_s with K_T leads to the difficulties of interpretation of their difference as a lifetime of the source $\tau=\sqrt{R_o^2-R_s^2}$. However, comparing the two EOS for $K_T \lesssim 2$ GeV we find a slightly larger τ for the pure hadronic gas EOS. This corresponds to the faster cooling of the QGP from the T_{in} to T_c, while preserving the total lifetime. On the other hand, the HBT radii reveal a much stronger dependence on the initial conditions: for the high K_T region the longitudinal correlation radius is smaller for the case of a smaller initial time.

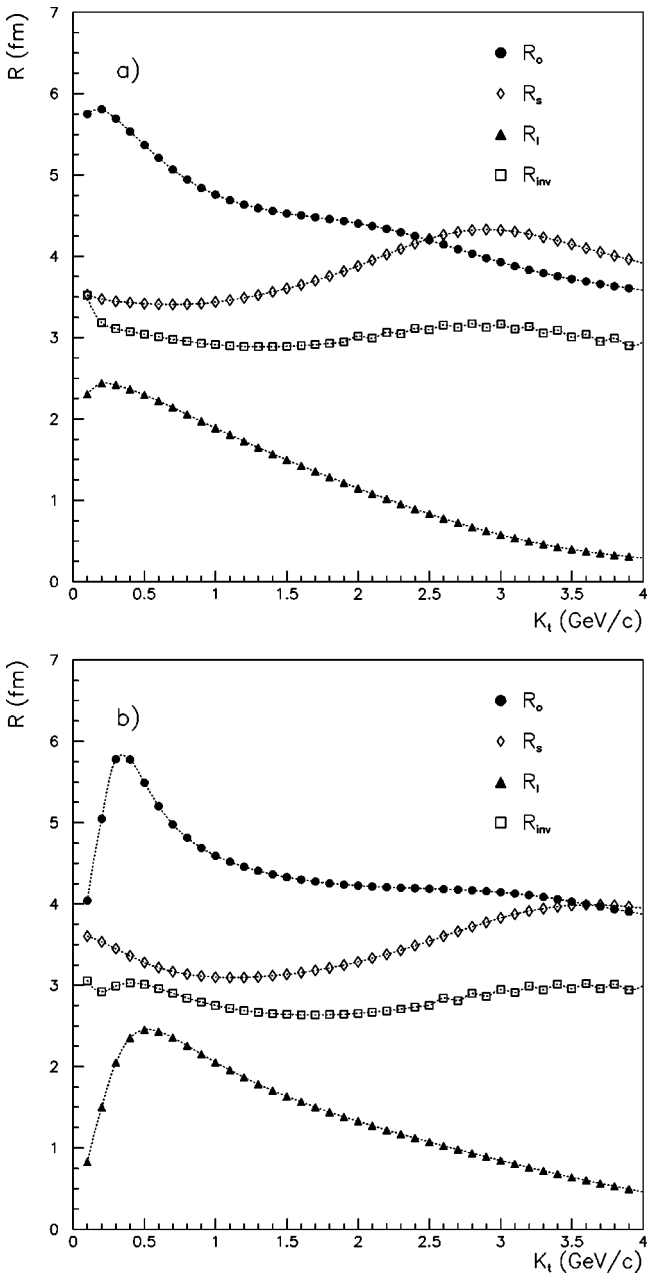

FIG. 5. HBT radii R_{out} (circles), R_{side} (diamonds), R_{long} (triangles), and R_{inv} (boxes) as functions of the total transverse momentum, calculated in central Pb+Pb collisions at SPS energy for the EOS including the phase transition [plot (a)] and pure hadronic gas [plot (b)].

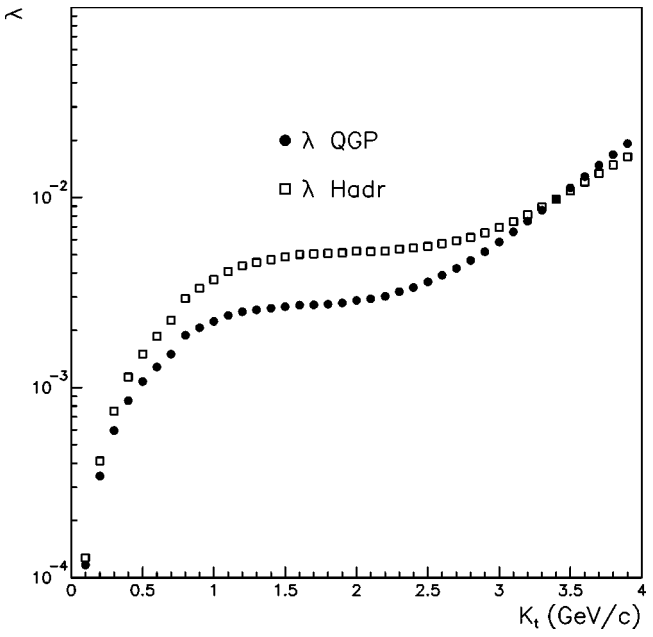

FIG. 6. "Correlation strength" parameter in central Pb+Pb collisions as SPS energy, calculated for the EOS including the phase transition (QGP) and pure hadronic gas (Hadr) EOS.

As was already mentioned, the invariant radius R_{inv} provides only averaged information of R_o, R_s, and R_l. One can see (Fig. 5), that this radius is insensitive to the changing of the EOS and initial condition of hydrodynamics.

Considering the "correlation strength" parameters (Fig. 6), one should remember that their absolute values should be taken with care especially at small $K_T \lesssim 2$ GeV/c as far as both predictions of the yield of prompt photons and emission rates of thermal photons are not well known at this region, and we used an extrapolation of the existing calculations. For $K_T \sim 2$ GeV/c, where predictions of the emission rate are more or less reliable, we find the correlation strength parameter on the level of 5×10^{-3}, which is accessible within the accuracy of the WA98 experiment [10].

Knowing the evolution of hot matter, we calculate as well the correlation functions of final pions. Then, accounting for correlations between neutral pions, we calculate the residual correlations of decay photons. We present the "all photon" correlation function, calculated for the case of the EOS including the phase transition, in Fig. 7. In this calculation we set the correlation strength parameter of final pions to 1. Thus we estimate the upper limit of the contribution of the residual correlations into photon correlations and find that even in this case one can disentangle correlations of direct photons and residual correlations. However, our calculations show that pions produced directly in the hot zone contribute $\sim 15\%$ to the total pion yield, while the rest are products of the decays of upper resonances. Therefore, in reality the contribution of the residual correlation to the photon correlations will be much smaller.

Now we switch to the RHIC energy. As for SPS energy we choose initial conditions of hydrodynamics so that we reproduce the spectrum of the final pions [18]. For the RHIC energy we consider only the EOS including the phase transition. For this EOS we fix the initial conditions $T_{in} = 400$ MeV and $\tau_{in} = 0.45$ fm/c. Repeating the same procedure as for the SPS energy, we extract the HBT parameters as a function of K_T — see Fig. 8.

Comparing this result with predictions for the SPS energy, one can see that the parameters R_o and R_s are almost the same, but at the RHIC energy R_s increases with K_T faster due to the larger radial collective velocity. In addition R_l exceeds at small K_T the corresponding radius predicted for the SPS energy. This is a result of a longer lifetime of the hot matter and larger final longitudinal source size. The calcu-

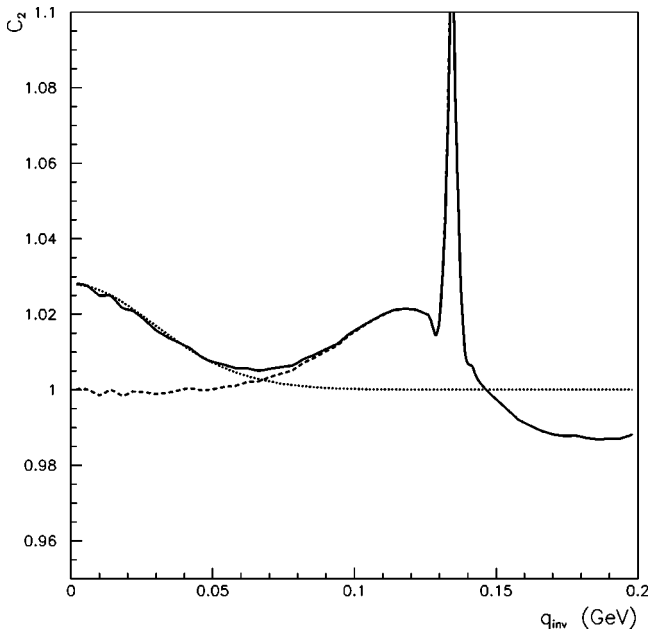

FIG. 7. Correlation function of photons in central Pb+Pb collision at SPS energy calculated with the EOS including the phase transition. Dotted line: correlation of direct photons. Dashed line: residual correlations due to π^0 correlations. Solid line: total photon correlation function.

lated correlation functions agree with previous estimations [3,4], although for small $K_T \sim 1$ GeV our radii are 20% larger.

As for the correlation strength parameter (see Fig. 9), it is approximately on the same level as in the SPS case, and

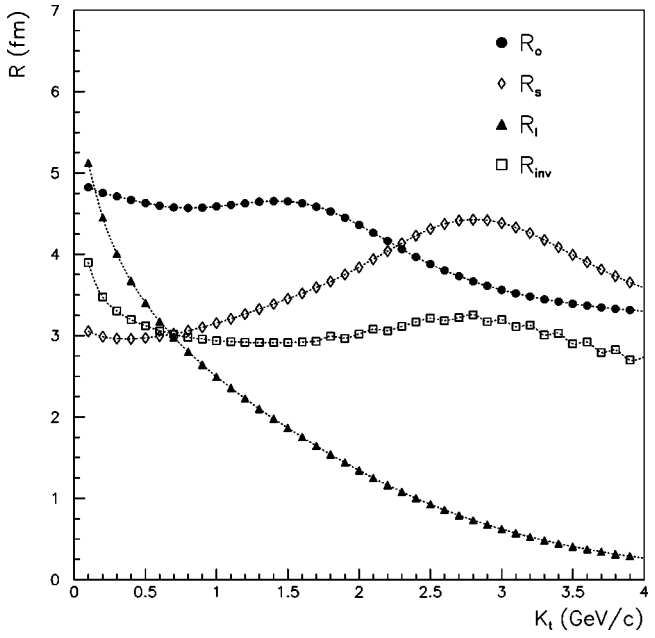

FIG. 8. HBT radii R_{out} (circles), R_{side} (diamonds), and R_{long} (triangles) as a function of total transverse momentum in central Au+Au collisions at RHIC energy calculated for the EOS including the phase transition.

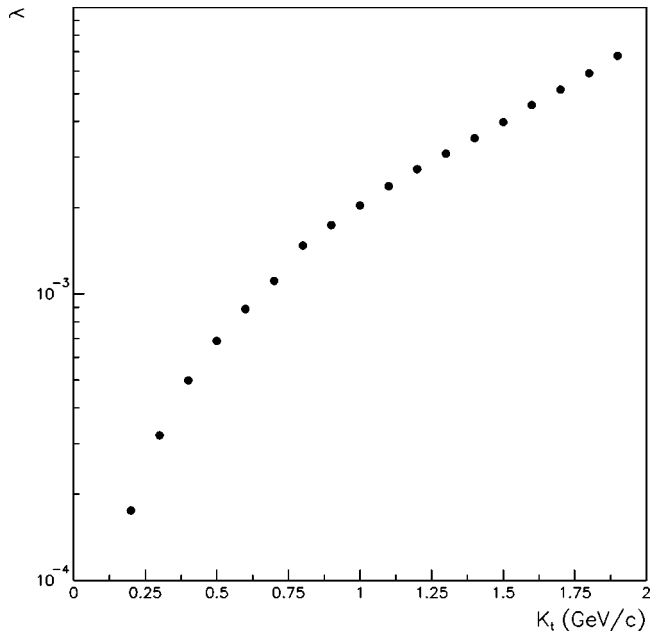

FIG. 9. Correlation strength parameter in central Au+Au collisions at RHIC energy calculated with the EOS including the phase transition.

therefore one can expect that the two-photon correlation function can be measured at RHIC energy in the PHENIX experiment.

VI. CONCLUSION

We analyzed the possibility of the measurement of HBT correlations in the photon-photon channel in the high multiplicity environment of heavy ion collisions. We demonstrated that correlations of direct photons can be disentangled from the residual correlations of decay photons. The latter do not contribute to the region of small invariant relative momentum $q_{inv} \lesssim 50$ MeV/c, and moreover, residual correlations of decay photons have wavelike shape, which facilitates the disentangle.

We evaluated *total* two-photon correlation functions in Pb+Pb collisions at the SPS energy. The extracted HBT radii do not reveal a dependence on the EOS, but rather on the initial conditions of the hydrodynamic model. We analyzed ''correlation strength'' parameters for SPS and RHIC energies and found that these measurements are possible in the frame of the WA98 and PHENIX experiments.

The strength of the correlation can be related to the ratio $(dN_\gamma^{direct}/dK_T)/(dN_\gamma^{total}/dK_T)$. and can be used as an independent method of measurement of direct photon yield especially at small transverse momenta of photons.

ACKNOWLEDGMENTS

The author would like to thank Yves Schutz for discussions and SUBATECH for hospitality during this work. This research was supported by Grant No. RFBR 00-15-96590.

APPENDIX: DERIVATION OF THE RELATION BETWEEN PHOTON AND PION CORRELATIONS

Here we present details of the evaluation of the relation between the distribution over the invariant relative momentum of neutral pions $dN^{\pi\pi}/dQ$ and the distribution of the daughter photons $dN^{\gamma\gamma}/dq$. We start from the general expression (5). As far as it is Lorenz invariant, we can evaluate the integral in any convenient reference frame. Let us go to the pion c.m. frame and take the polar axis along $\vec{p}_1$ and the azimuthal angle account from $\vec{k}_1$. Using the identity $\delta(k-\cdots)d^3k/\omega=\delta(k^2)\ \theta(\omega)$, we obtain

$$\frac{dN^{\gamma\gamma}}{dq}=\frac{q}{2^5\ \pi^3}\int d\omega_1\ dc_1,\ d\omega_3\ dc_3\ d\phi_3\ \omega_1\ \omega_3\ \theta(\omega_2)\times\theta(\omega_4)\,\delta(q^2+(k_1-k_3)^2)\ \delta(k_2^2)\ \delta(k_4^2)\ \frac{dN^{\pi\pi}}{dQ}dQ, \tag{A1}$$

where $c_1\equiv\cos\theta_1$ and $c_3\equiv\cos\theta_3$, and we denote the last line in Eq. (5) as the distribution of pion pairs over the invariant relative momentum $Q=\sqrt{-(p_1-p_2)^2}$:

$$\frac{dN^{\pi\pi}}{dQ}\equiv\int\ \frac{d^3p_1}{2\ \varepsilon_1\ (2\pi)^3}\frac{d^3p_2}{2\ \varepsilon_2\ (2\pi)^3}\ \delta(Q-\sqrt{-(p_1-p_2)^2})\times f(p_1)f(p_2)C_2(p_1,p_2). \tag{A2}$$

Using the δ functions in Eq. (A1) we integrate over c_1, c_3, and ϕ_3:

$$\frac{dN^{\gamma\gamma}}{dq}=\frac{q}{2^7\ \pi^3}\int d\omega_1\ d\omega_3\ \theta(\omega_2)\ \theta(\omega_4)\ \theta(1-\overline{c_1^2})\times\theta(1-\overline{c_3^2})\frac{\theta(1-\overline{\cos\phi_3{}^2})}{p^2\ \omega_1\ \omega_3\ |\overline{s_1}\ \overline{s_3}\ \overline{\sin\phi_3}|}\frac{dN^{\pi\pi}}{dQ}dQ, \tag{A3}$$

where

$$\overline{c}_1=-\frac{m^2-2\varepsilon\omega_1}{2p\omega_1},$$

$$\overline{c}_3=\frac{m^2-2\varepsilon\omega_3}{2p\omega_3},$$

$$\overline{\cos\phi_3}=-\frac{q^2-2\omega_1\omega_3(1-\overline{c}_1\overline{c}_3)}{2\omega_1\omega_3\overline{s}_1\overline{s}_3},$$

$$\varepsilon_1=\varepsilon_2=\varepsilon=\frac{1}{2}\sqrt{Q^2+4m^2},$$

$$p_1=p_2=p=\frac{1}{2}Q.$$

Let us rewrite the denominator in Eq. (A3):

$$p^2\omega_1\omega_3|\overline{s_1}\overline{s_3}\overline{\sin\phi_3}|=p^2\omega_1\omega_3\{(1-\overline{c_1^2})(1-\overline{c_3^3})(1-\overline{\cos\phi_3}^2)\}^{1/2}=\frac{p}{2}\{a\omega_3^2+b\omega_3+c\}^{1/2}, \tag{A4}$$

where

$$a=-(4\varepsilon\omega_1-m^2)^2,$$

$$b=4m^2\varepsilon\omega_1^2+(2q^2p^2-m^4+2q^2\varepsilon^2)\omega_1-q^2m^2\varepsilon,$$

$$c=-m^4\omega_1^2-2q^2m^2\varepsilon\omega_1-q^4p^2+q^2m^4.$$

Now let us consider the limits. One can find that the limit $\theta(1-\overline{c_3^2})$ is more severe than $\theta(\omega_4)\equiv\theta(\varepsilon-\omega_3)$. In addition, one can see that the polynomial under the square root in Eq. (A4) is positive in several regions of the $\omega_1-\omega_3$ plane, one of which exactly coincides with the region defined by the set of conditions $\theta(1-\overline{c_1^2})\ \theta(1-\overline{c_3^2})\ \theta(1-\overline{\cos\phi_3}^2)$ and others excluded by these conditions. Therefore, the integration over ω_3 in Eq. (A3) should be taken between the roots of the polynomial. The result is

$$\frac{dN^{\gamma\gamma}}{dq}=\frac{q}{2^6\pi^2}\int d\omega_1\frac{\theta(1-\overline{c_1^2})\,\theta(\Delta)}{|4\varepsilon\omega_1-m^2|p}\frac{dN^{\pi\pi}}{dQ}dQ, \tag{A5}$$

where Δ is the discriminant of the polynomial:

$$\Delta=m^4q^2\varepsilon(\varepsilon+p-2\omega_1)(\varepsilon-p-2\omega_1)\left(\frac{m^2+q^2}{\varepsilon}-4\omega_1\right).$$

Integrating over ω_1 in the limits so that $\Delta>0$ and $|\overline{c_1}|<1\Leftrightarrow\omega_1^{min}<\omega_1<\omega_1^{max}$, where

$$\omega_1^{min}=\begin{cases}(\varepsilon-p)/2, & q<\varepsilon-p,\\ (q^2+m^2)/4\varepsilon, & q\geqslant\varepsilon-p,\end{cases}\qquad \omega_1^{max}=\frac{\varepsilon+p}{2},$$

we obtain

$$\frac{dN^{\gamma\gamma}}{dq}=\frac{q}{2^7\pi^2}\int dQ\frac{dN^{\pi\pi}}{dQ}\frac{\theta(\varepsilon+p-q)}{p\varepsilon}\times\left\{\ln\left[\frac{\varepsilon+p}{\varepsilon-p}\right]+\min\left(0,\ln\left[\frac{\varepsilon-p}{q}\right]\right)\right\}. \tag{A6}$$

[1] See, e.g., reviews in the recent Quark Matter conferences: Nucl. Phys. **A698**, 1 (2002); **A661**, 1 (1999); **A638**, 1 (1998).
[2] M. Marques *et al.*, Phys. Rep. **284**, 91 (1997); Phys. Rev. Lett. **73**, 34 (1994); Phys. Lett. B **349**, 30 (1995).
[3] D.K. Srivastava and J.I. Kapusta, Phys. Lett. B **307**, 1 (1993); Phys. Rev. C **48**, 1335 (1993); **50**, 505 (1994).
[4] A. Timmermann, M. Plumer, L. Razumov, and R.M. Weiner, Phys. Rev. C **50**, 3060 (1994).
[5] U. Wiedemann and U. Heinz, Phys. Rep. **319**, 145 (1999).
[6] D. Neuhauser, Phys. Lett. B **182**, 289 (1986).
[7] L.V. Razumov and H. Feldmeier, Phys. Lett. B **377**, 129 (1996).
[8] C. Slotta and U. Heinz, Phys. Lett. B **391**, 469 (1997).
[9] R.M. Weiner, hep-ph/9809202.
[10] M.M. Aggarwal *et al.*, Nucl. Phys. **A685**, 399 (2001).
[11] A. Deloff and T. Siemiarczuk, Nucl. Instrum. Methods Phys. Res. A **427**, 607 (1999).
[12] T. Peitzmann, Z. Phys. C **54**, 559 (1992).
[13] D. Peressounko (unpublished).
[14] D. Peressounko and Yu. Pokrovsky, hep-ph/0009025.
[15] J. Kapusta *et al.*, Phys. Rev. D **44**, 2774 (1991).
[16] P. Arnold, G.D. Moore, and L.G. Yaffe, J. High Energy Phys. **12**, 009 (2001).
[17] L. Xiong *et al.*, Phys. Rev. D **46**, 3798 (1992).
[18] PHENIX Collaboration, Adcox *et al.*, Phys. Rev. Lett. **88**, 022301 (2002).
[19] D.K. Srivastava, Phys. Rev. D **49**, 4523 (1994), D.K. Srivastava and C. Gale, Phys. Lett. B **319**, 407 (1993).